Research Article

The Adsorption Capacity, Pore Structure, and Thermal Behavior of the Modified Clay Containing SSA

Haijun Lu, Qian Zhang, Yiqie Dong, Jixiang Li, and Xiong Zhang

Institute of Poromechanics, Wuhan Polytechnic University, Wuhan 430023, China

Correspondence should be addressed to Haijun Lu; lhj_whpu@163.com

Sewage sludge ash (SSA) was created by burning municipal sludge. The potential of clay containing 1 or 3 or 5% SSA was assessed for use as a landfill liner-soil material. Batch adsorption, low temperature N_2 adsorption, and TG-DTA tests were performed to evaluate the adsorption capacity, micropore structure, thermostability, and components of soils under Cr(VI) and Pb(II) chemical solutions. With the increasing amount of SSA in modified clay, the adsorption capacity of Cr(VI) and Pb(II) to the modified clay increases gradually. After absorption, the pore size of modified clay ranges from 2 nm to 8 nm. With the increasing amount of absorption, the pore volume decreases and the specific surface area increases. With the increasing of adsorption concentration of Cr(VI) and Pb(II), the mass loss percentage of modified clay increases to 23.4% and 12.6%, respectively. The modified clay containing SSA may be used as a good barrier material to attenuate contamination of Cr(VI) and Pb(II) in landfills.

1. Introduction

Leachate from solid-waste landfills was found to contain a number of heavy metal ions. These heavy metal ions may enter the aquifer underlying the landfill and thereby pose a potential threat to human health [1–3]. To prevent the transport of contaminants present in the leachate, the liner system composed of the compacted clay is widely applied to design of the landfill [4]. However, many heavy metal ions can pollute groundwater by diffusion through a block liner. Hence, there is a crucial need for the development of a new landfill liner that can effectively prevent the transport of heavy metal ions [5, 6].

Sewage sludge is the inevitable by-product of sewage deposition. Currently, the global annual output of wet sewage [7] is 2.241×10^{-7} t. Wet sewage is usually disposed by concentrate dewatering and then stored in security landfills. In addition to a few organic substances, wet sewage contains inorganic substances [8–10] that are rich in silicon and aluminum. Studies show that dewatered sludge can be transformed into granular ash after high temperature burning. Granular ash is a porous material [11–13] with a high specific surface area and ion-exchange capacity. Granular ash is considered a mineral admixture, which enhances

the mechanical properties of concrete. Granular ash mixed with clay can be used as a modified landfill liner material that can absorb pollutants in leachate. However, studies have not been conducted on this material.

This study aims to evaluate the adsorption capacity, pore structure, and phase composition of modified clay as new landfill liner material. Batch adsorption tests were used to explore the adsorption capacity of Cr(VI) and Pb(II) to the modified clay and decide the additive amount of sewage sludge ash (SSA). Low temperature N_2 adsorption tests were used to analyze pore structure of the modified clay. TG-DTA tests were performed to explore the thermostability and components of the modified clay.

2. Testing Materials and Methods

2.1. Testing Materials. The clay and sewage sludge used in the tests are obtained from a construction site and the Hanxi sewage treatment plant in Wuhan, China, respectively. Clay was dug from a depth of 2.5~3.0 m. The soil was kept in a sealed bag to avoid contamination. The basic physical properties of the clay are listed in Table 1, and the chemical compositions of the clay are listed in Table 2. This type of

TABLE 1: The basic physical properties of the clay in the tests.

Proportion	Specific surface area/m^2/g	Natural moisture content/%	W_L/%	W_P/%	I_P	Particle size distribution/%			
						>0.05 mm	0.05~0.005 mm	0.005~0.002 mm	<0.002 mm
2.65	86.53	21.2	48.5	26.2	22.3	12	32	45	11

TABLE 2: The chemical compositions of clay.

SiO_2	Al_2O_3	Fe_2O_3	CaO	MgO	K_2O	Na_2O
58.42	25.23	0.24	0.51	0.12	5.32	2.67

sewage sludge is dehydrated by machinery. On the basis of "Determination Method for Municipal Sludge in Wastewater Treatment Plant" (CJ/T 221-2005), the basic property indexes of sewage sludge are shown in Table 3.

Sewage sludge was kept in a thermostatic temperature dry box at 105°C for 24 h. After 24 hours, the sewage sludge was weighed every 2 hours. The weighing of the samples was continued until the quality difference is less than 0.1% of the total quality. At that time, the samples can be considered to be completely free of water. The samples were broken into pieces and sieved through a 2-mesh screen. Thereafter, the samples were placed in the muffle furnace. The burning temperature was set at 850°C. The samples were stirred every 24 hours to achieve even heating [14]. After 1 week, the samples turned into grainy red brown ash. The red brown ash was sieved through a 200-mesh screen and then hermetically sealed for later use. The chemical constituents of sewage sludge ash (SSA) are listed in Table 4. The microstructure, pore volume, and pore size distribution of SSA are shown in Figures 1 and 2. These figures show that the SSA is porous and that every relic has a small volume. The pore volume distribution of SSA is uniform, with a high proportion of 2 nm to 4 nm pores.

2.2. Testing Methods

2.2.1. Batch Adsorption Tests.
The modified clay was composed of 1% SSA plus 99% clay or 3% SSA plus 97% clay or 5% SSA plus 95% clay. Dry soil samples of 12.5 g were soaked in 50 mL $K_2Cr_2O_7$ and $PbCl_2$ chemical solutions, respectively. The initial Cr(VI) and Pb(II) concentration was 0–300 mg/L. After stirring evenly, the mixture was placed in a water bath instrument under a temperature of 25°C. The concentration of Cr(VI) and Pb(II) in the suspension solution after centrifugation was measured by spectrophotometry (Shanghai Third Analytical Instruments Factory) according to GB 7467-87 DPC. The error of the colorimetric measurements was less than 4%. Each batch test was repeated three times.

The concentration of heavy metal ions adsorbed on the soil was calculated from the mass balance:

$$C_s = \frac{(C_0 - C_e) V}{M}, \tag{1}$$

where C_s is the amount of Cr(VI) and Pb(II) adsorbed onto the soil samples, C_0 is the initial concentration of Cr(VI) and Pb(II), C_e is equilibrium aqueous concentration of Cr(VI)
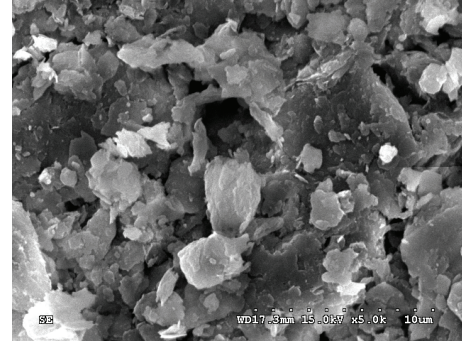

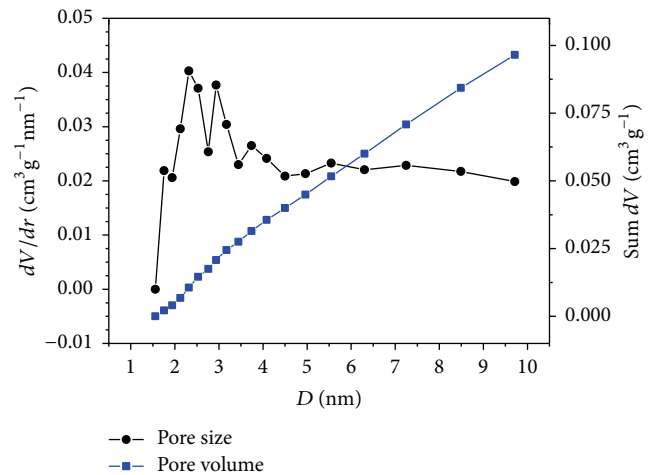FIGURE 1: The microstructure of SSA.

FIGURE 2: The pore volume and pore size distributions of SSA.

and Pb(II), V is the volume of the aqueous phase, and M is the weight of the soil samples.

2.2.2. The Low Temperature N_2 Adsorption Tests.
Modified clay containing 3% SSA polluted by 0, 100, and 250 mg/L of Cr(VI) and Pb(II) solutions was used in this test. The samples of 0.2 g were used in the low temperature N_2 adsorption tests. The JW-BK static N_2 adsorption instrument was used to test the pore structure of the sample. The absorbing medium of the test was 99.99% N_2, and the sample was kept at liquid nitrogen saturation temperature. The relative pressure P/P_0 ranged from 0.01 to 0.995. The sample was adsorbed and desorbed isothermally at 22 pressure points. The specific surface area, the pore volume, and pore size distribution of samples were calculated according to the standard BET method [15].

TABLE 3: The basic physical property indexes of sewage sludge.

pH	Proportion (g/mL)	Organic matter content (%)	Moisture content (%)	Void ratio	Permeability coefficient (cm/s)	Compressive strength (kg/cm²)
6.96	1.24	43.2	80.3	3.36	1.20×10^{-8}	0.068

TABLE 4: The chemical properties of SSA.

SiO_2	Al_2O_3	Fe_2O_3	CaO	SO_3	P_2O_5	K_2O	MgO	TiO_2	Na_2O	Others
45.5%	16.6%	8.11%	6.64%	6.61%	5.72%	4.45%	3.90%	0.98%	0.83%	0.66%
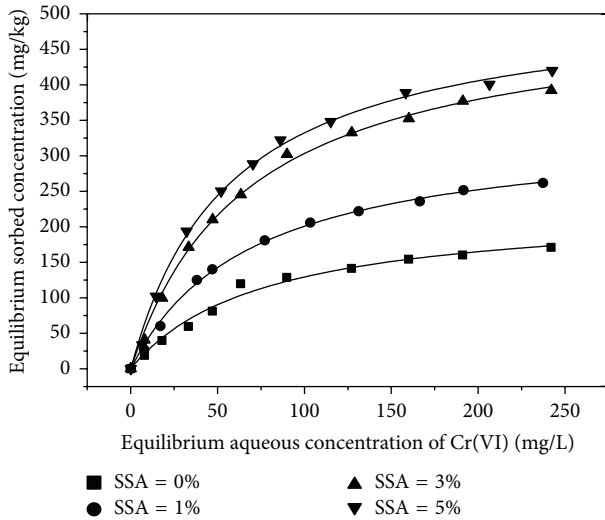
FIGURE 3: The adsorption isotherm for Cr(VI) with modified clay.

2.2.3. TG-DTA Tests. The samples were the same to the low temperature N_2 adsorption tests. Thermal gravimetric and differential thermal analyzer (Beijing Henven Scientific Instrument Factory) was used to test the endothermic-exothermic reaction, thermostability, and components of the sample. The temperature range of the thermal analyzer was 0~1000°C and the heating rate was controlled at 10°C/min.

3. Results and Discussion

3.1. Absorption Capacity. The adsorption isotherm for Cr(VI) and Pb(II) with modified clay are shown in Figures 3 and 4, and all adsorptions belong to the Langmuir isotherm model. The adsorption of Cr(VI) and Pb(II) onto the soil specimens was modeled as a Langmuir isotherm [16]. The values of the isotherm parameters are given in Table 5. With the content of SSA increasing from 0% to 3%, the adsorption capacity of Cr(VI) and Pb(II) to the modified clay increases dramatically. But when the content of SSA increased from 3% to 5%, the adsorption capacity shows a slow increase tendency. At C_0 being 250 mg/L, the adsorption of Cr(VI) and Pb(II) to modified clay containing 3% SSA is 392.25 and 602.04 mg/kg; these values were 2.30 or 1.88 times greater than that of the raw clay, respectively. SSA has loose structure and large porosity or specific surface area [17]. Hence, ionic charge can

TABLE 5: The isotherm parameter for Cr(VI) and Pb(II) with modified clay.

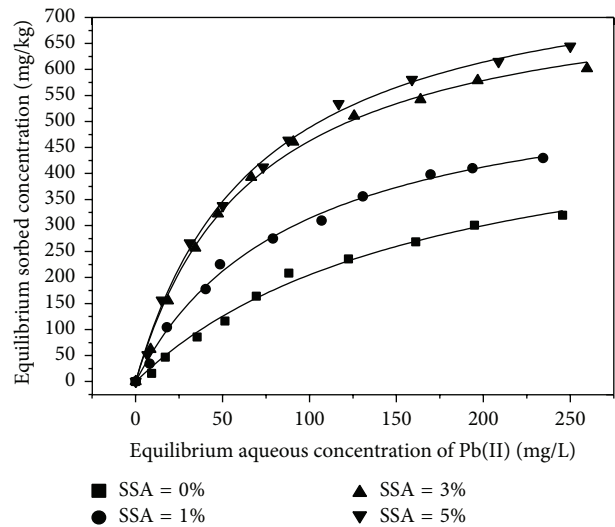| Ions		0%	1%	3%	5%
Cr(VI)	b (L/mg)	0.013	0.015	0.015	0.016
	q_m (mg/kg)	227.80	339.10	507.51	520.38
	R^2	0.986	0.998	0.997	0.997
Pb(II)	b (L/mg)	0.006	0.011	0.015	0.014
	q_m (mg/kg)	557.33	601.20	773.26	827.15
	R^2	0.992	0.996	0.997	0.997

FIGURE 4: The adsorption isotherm for Pb(II) with modified clay.

be adsorbed on the surface of SSA debris in the adsorption process. A large number of metal ions absorbed to the surface of the debris, resulting in a positive charge presented in debris. The heavy metal ion adsorption capacity of the debris gradually decreases under the action of Coulomb repulsion.

3.2. Pore Structure. The adsorption and desorption isotherm of the samples are shown in Figure 5. According to IUPAC classification, the isotherm is IV category. There is a H_3 hysteresis loop in the process of adsorption and desorption [18]. The bottle shaped pore of the soil is rough, and absorbed N_2 can be easily blocked in the orifice. Thus, N_2 cannot overflow completely in the desorption process [19].
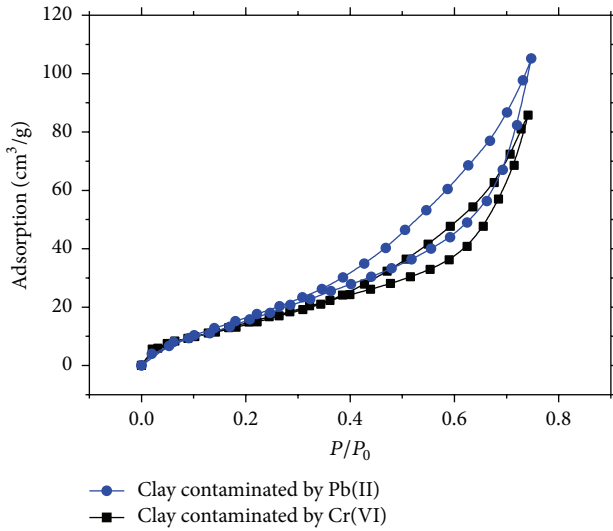
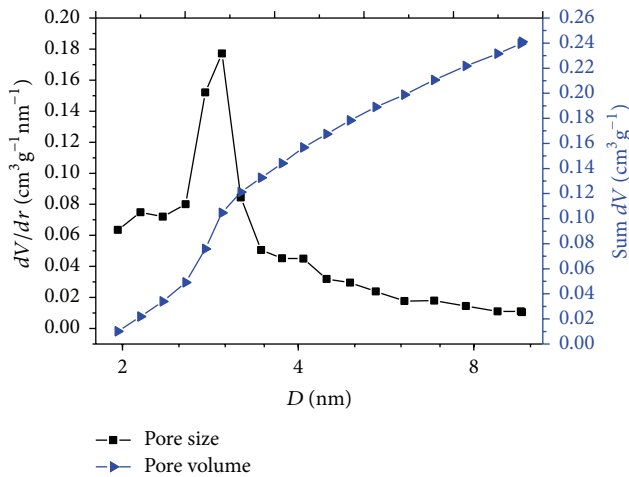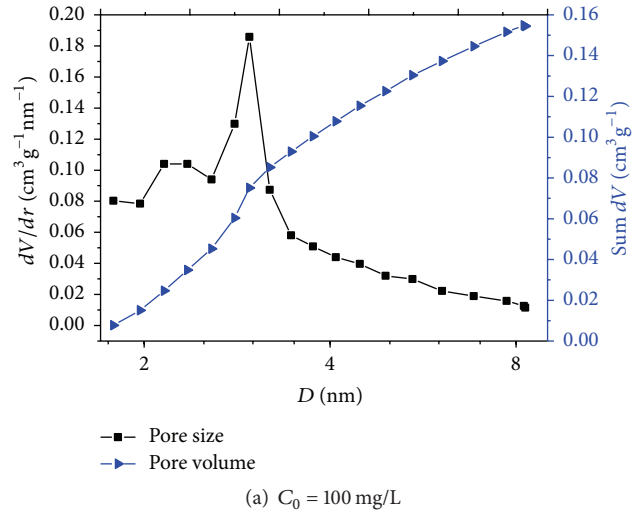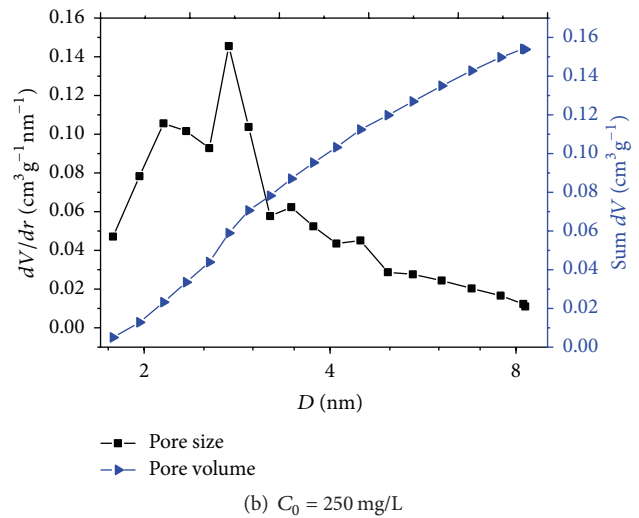FIGURE 5: Adsorption and desorption isotherm of the samples.

FIGURE 6: The pore volume and pore size distributions of modified clay ($C_0 = 0$ mg/L).

(a) $C_0 = 100$ mg/L

(b) $C_0 = 250$ mg/L

FIGURE 7: The pore volume and pore size distributions of modified clay after absorbing Cr(VI).

The pore volume and pore size distribution of modified clay are shown in Figures 6–8. The pore distribution of modified clay is mostly in the range of mesoporous pore size (2~8 nm) [20]. In the 2.5~3.5 nm range, the peak value of the mesopore is relatively large. After Pb(II) and Cr(VI) being absorbed by the samples, the proportion of the mesopore (2~2.5 nm) increases, and the number of mesopore (>3.5 nm) decreased. At the same time, the double peak phenomenon occurs.

The pore parameter of samples can be seen at Table 6. The relation between the pore parameter and adsorption capacity of Pb(II) and Cr(VI) can be seen in Figure 9. The total pore volume dramatically decreased to stable values with increasing adsorption capacity. The specific surface area shows the opposite trend. Ions will be closely packed on the inner wall of pore in the adsorption process, resulting in increasing of the inner wall surface roughness and decreasing the total pore volume.

3.3. Thermostability and Components.
The DTG-T curves of samples are shown in Figure 10. The weight loss of the samples is shown in Table 7. Due to the removal of free water and weakly bound water in samples, there is an obvious weight loss valley at 25~250°C. Another weight loss valley appears at 400~700°C owing to the reduction reaction of metal ions. The weight loss valley becomes obvious with the increasing of adsorption capacity of Cr(VI) and Pb(II) onto the samples. Metal ions need absorb heat to obtain electrons in the process of reduction reaction [21]. The valence of Cr(VI) and Pb(II) declines and they transformed into mental element. The maximum temperature is 1000°C in the test. The temperature did not reach the melting point of Cr or Pb element. Metal elements are closely attached to the soil particles. At 700~1000°C, the material decomposition reaction is gradually completed, and the weight loss of samples is less than 0.2%.

The DTA-T curves of the samples are shown in Figure 11. The endothermic valley and the exothermic peak are shown in the DTA-T curve. The absorption valley of the curve will appear, indicating the samples need absorb heat in

TABLE 6: Pore parameter of the samples.

Sample classification	Initial concentration of Cr(VI) and Pb(II)	The total pore volume (cm³/g)	Average pore size (nm)	Specific surface area (m²/g)
Modified clay	0 mg/L	0.241	5.673	104.98
Modified clay after absorbing Cr(VI)	100 mg/L	0.154	5.086	107.17
	250 mg/L	0.147	5.038	118.60
Modified clay after absorbing Pb(II)	100 mg/L	0.145	4.718	126.20
	250 mg/L	0.139	4.655	137.14

TABLE 7: Percentage of weight loss.

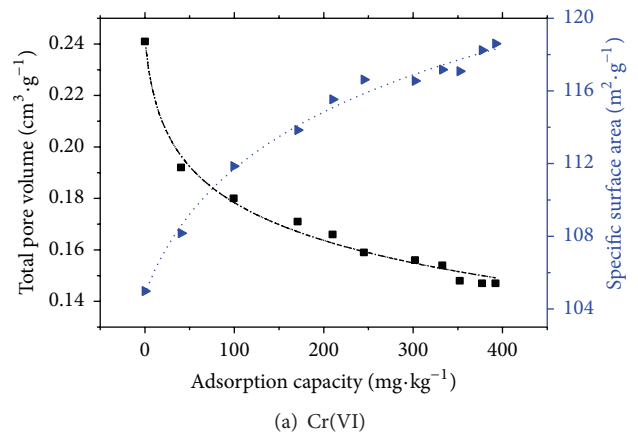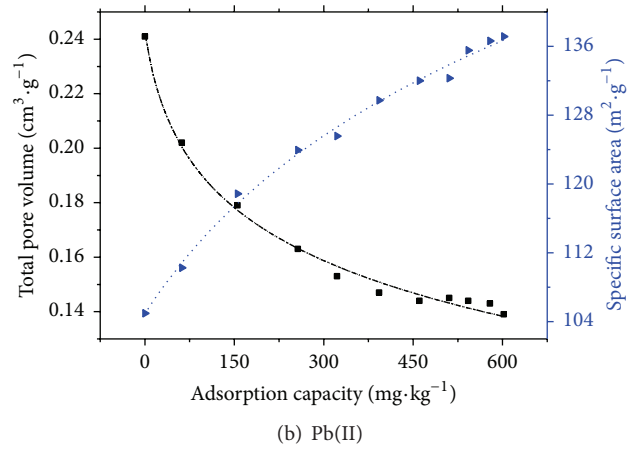| Anaerobic fermentation	25~250°C	250~400°C	400~700°C	>700°C	Total weight loss
0 mg/L	9.40%	0.46%	2.69%	0.19%	12.74%
$C_{Cr(VI)} = 100$ mg/L	9.34%	0.60%	2.82%	0.15%	12.91%
$C_{Cr(VI)} = 250$ mg/L	11.47%	0.54%	3.32%	0.06%	15.39%
$C_{Pb(II)} = 100$ mg/L	9.32%	0.46%	2.78%	0.15%	12.71%
$C_{Pb(II)} = 250$ mg/L	10.63%	0.45%	3.03%	0.16%	14.27%
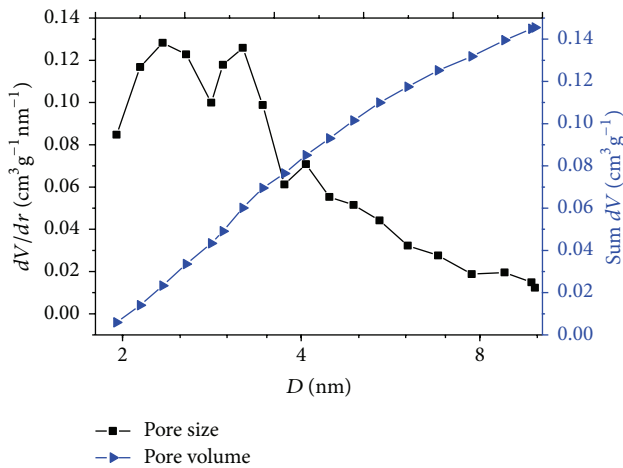
(a) $C_0 = 100$ mg/L
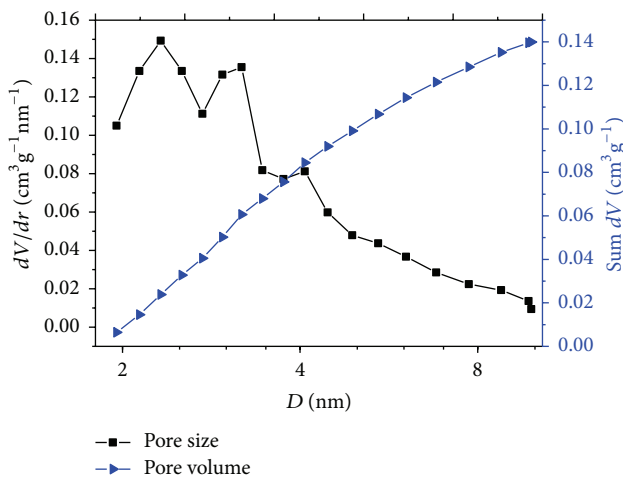
(b) $C_0 = 250$ mg/L

FIGURE 8: The pore volume and pore size distributions of modified clay after absorbing Pb(II).
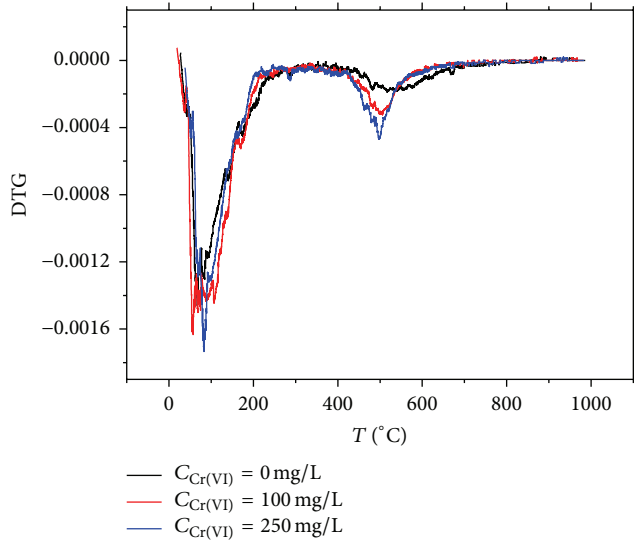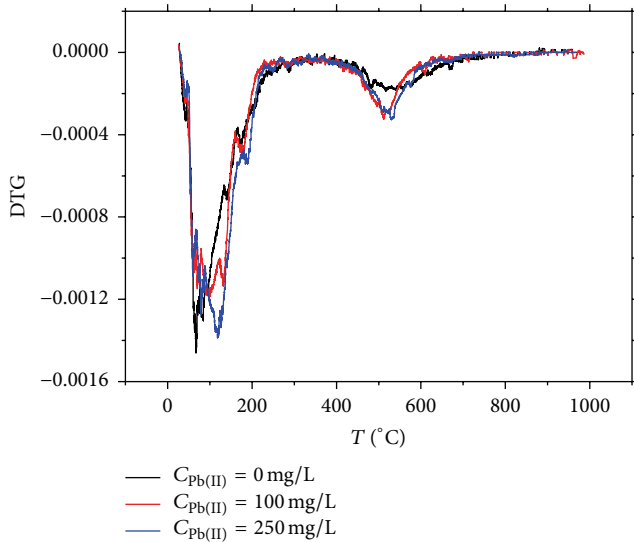

(a) Cr(VI)

(b) Pb(II)

FIGURE 9: Adsorption equilibrium concentration and parameter variation curve of pore structure.

the dehydration. An exothermic peak can be found in the combustion and oxidative cleavage reaction. Because of the dehydration reaction of free water and weakly bound water,
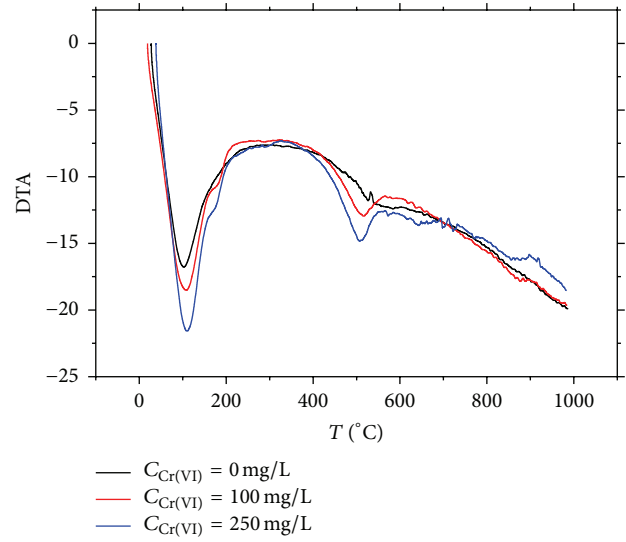
FIGURE 10: Derivation thermogravimetry curvilinear (DTG/TG-T curvilinear).

FIGURE 11: Differential thermal analysis curvilinear (DTA-T curvilinear).

a large endothermic valley will appear at 25~250°C. Another endothermic valley occurs owing to reduction reaction of metal ions at 400~700°C.
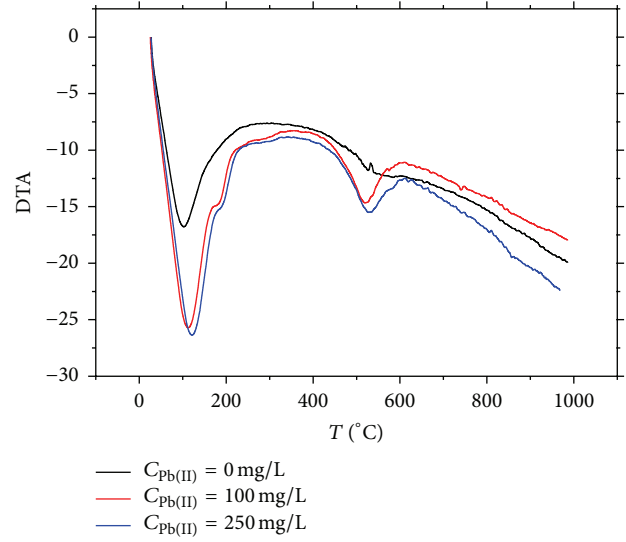
4. Conclusions

To evaluate the feasibility of modified clay containing SSA as a new landfill liner-soil material, the adsorption capacity of Cr(VI) and Pb(II) to modified clay was observed by the batch adsorption tests. The pore structure, thermostability, and components of the modified clay were observed by low temperature N_2 adsorption tests and TG-DTA tests. Based on these experiments the following conclusions can be drawn:

(1) The adsorption capacity of Cr(VI) and Pb(II) onto modified clay containing SSA was more obvious than

that of raw clay. The adsorption model is Langmuir isotherm.

(2) The adsorption and desorption isotherms of modified clay polluted by Cr(VI) and Pb(II) belong to IV category, and an H_3 hysteresis loop exists. The pores of the samples are mainly composed of the mesopore (2~8 nm). With the increasing of adsorption capacity, the pore volume dramatically decreases to certain value, and the specific surface area increases.

(3) Due to the removal of free water or weakly bound water and the reduction reaction of metal ions, the DTG-T or DTA-T curves of the samples show two obvious weight loss or endothermic valley at 25~250°C and 400~700°C, respectively.

(4) SSA is a kind of potential material for use as sorptive amendment for trapping heavy metals in clay landfill liners.
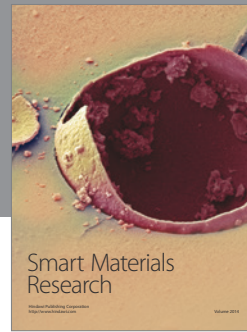
Competing Interests

The authors declare that they have no competing interests.

Acknowledgments

References

[1] P.-J. He, Z. Xiao, L.-M. Shao, J.-Y. Yu, and D.-J. Lee, "In situ distributions and characteristics of heavy metals in full-scale landfill layers," *Journal of Hazardous Materials*, vol. 137, no. 3, pp. 1385–1394, 2006.

[2] A. Giannis, G. Makripodis, F. Simantiraki, M. Somara, and E. Gidarakos, "Monitoring operational and leachate characteristics of an aerobic simulated landfill bioreactor," *Waste Management*, vol. 28, no. 8, pp. 1346–1354, 2008.

[3] X. Qu, P.-J. He, L.-M. Shao, and D.-J. Lee, "Heavy metals mobility in full-scale bioreactor landfill: initial stage," *Chemosphere*, vol. 70, no. 5, pp. 769–777, 2008.

[4] J.-L. Zhang, M.-T. Luan, and Q. Yang, "Numerical analysis of transport of landfill pollutants in unsaturated soil layer," *Chinese Journal of Geotechnical Engineering*, vol. 28, no. 2, pp. 221–224, 2006.

[5] H. J. Lu, M. T. Luan, and J. L. Zhang, "Study on transport of Cr(VI) through the landfill liner composed of two-layer soils," *Desalination*, vol. 266, no. 1–3, pp. 87–92, 2011.

[6] H. Lu, M. Luan, and J. Zhang, "Transport of Cr(VI) through clay liners containing activated carbon or acid-activated bentonite," *Applied Clay Science*, vol. 50, no. 1, pp. 99–105, 2010.

[7] S. J. Hang, X. D. Liu, and P. Liang, "Misunderstanding of sludge disposal and treatment and control strategy," *China Water & Wastewater*, vol. 20, no. 12, pp. 89–92, 2004.

[8] P. Chen, L. T. Zhan, and W. Wilson, "Experimental investigation on shear strength and permeability of a deeply dewatered sewage sludge for use in landfill covers," *Environmental Earth Sciences*, vol. 71, no. 10, pp. 4593–4602, 2014.

[9] A. Biasin, M. Della Zassa, M. Zerlottin, D. Refosco, R. Bertani, and P. Canu, "On the understanding and control of the spontaneous heating of dried tannery wastewater sludge," *Waste Management*, vol. 34, no. 4, pp. 817–824, 2014.

[10] J. Zou, Y. Dai, K. Pan et al., "Recovery of silicon from sewage sludge for production of high-purity nano-SiO2," *Chemosphere*, vol. 90, no. 8, pp. 2332–2339, 2013.

[11] H. F. Wang, J. J. Lu, K. F. Chen, and H. L. Duan, "Harmless treatment of used foundry sands and dewatered municipal sludge by microwave," *Metalurgija*, vol. 54, no. 3, pp. 459–461, 2015.

[12] S. Ghosh, S. Mukherjee, A. Z. Al-Hamdan, and K. R. Reddy, "Efficacy of fine-grained soil as landfill liner material for containment of chrome tannery sludge," *Geotechnical and Geological Engineering*, vol. 31, no. 2, pp. 493–500, 2013.

[13] C. Vogel, R. M. Exner, and C. Adam, "Heavy metal removal from sewage sludge ash by thermochemical treatment with polyvinylchloride," *Environmental Science and Technology*, vol. 47, no. 1, pp. 563–567, 2013.

[14] R. Li, W. Zhao, Y. Li, W. Wang, and X. Zhu, "Heavy metal removal and speciation transformation through the calcination treatment of phosphorus-enriched sewage sludge ash," *Journal of Hazardous Materials*, vol. 283, pp. 423–431, 2015.

[15] S. T. Pham and W. Prince, "Effects of carbonation on the specific surface BET of cement mortar measured by two different methods: Nitrogen adsorption and water adsorption," *Advanced Materials Research*, vol. 931-932, pp. 421–425, 2014.

[16] L. Y. Xie, L. A. Luo, and Z. Li, "Measurement and simulation of adsorption isotherms of VOCs on MAC," *Journal of Chemical Industry and Engineering*, vol. 57, no. 6, pp. 1357–1363, 2006.

[17] K.-L. Lin, W.-J. Huang, K.-C. Chen, J.-D. Chow, and H.-J. Chen, "Behaviour of heavy metals immobilized by co-melting treatment of sewage sludge ash and municipal solid waste incinerator fly ash," *Waste Management and Research*, vol. 27, no. 7, pp. 660–667, 2009.

[18] J.-P. Bellat, C. Paulin, M. Jeffroy et al., "Unusual hysteresis loop in the adsorption-desorption of water in NaY zeolite at very low pressure," *Journal of Physical Chemistry C*, vol. 113, no. 19, pp. 8287–8295, 2009.

[19] Y. T. Li, S. Y. Liu, X. L. Zhao, H. Chen, and D. Y. Wang, "Effect of straw-bentonite-polyacrylamide composites on nitrogen adsorption of sandy soil," *Transactions of the Chinese Society of Agricultural Engineering*, vol. 28, no. 7, pp. 111–116, 2012.

[20] D. Z. Borislav, J. C. Jiří, S. Martin, and J. Josef, "Pore classification in the characterization of porous materials: a perspective," *Central European Journal of Chemistry*, vol. 5, no. 4, pp. 385–395, 2007.

[21] A. Magdziarz and M. Wilk, "Thermogravimetric study of biomass, sewage sludge and coal combustion," *Energy Conversion and Management*, vol. 75, pp. 425–430, 2013.